Scientific
Research
Publishing

A-Site Effect on the Conversion of Bio-Ethanol into Isobutene over Ternary $A_1Zn_yZr_zO_n$ Catalysts

Feng Liu, Yong Men*, Jinguo Wang, Xiaoxiong Huang, Biao Zhao, Rong He

College of Chemistry and Chemical Engineering, Shanghai University of Engineering Science, Shanghai, China
Email: *men@sues.edu.cn

Abstract

Ternary multifunctional $A_1Zn_yZr_zO_n$ catalysts are prepared by introducing A-site transition metals with the redox capability into binary $Zn_1Zr_8O_n$. Structure and morphology were investigated by means of XRD, BET and FESEM, respectively. Activity data showed that Cr addition exhibited obvious beneficial effect to promote isobutene production from direct conversion of bio-ethanol compared to other A-site metal dopants. A significant higher yield of isobutene over Cr-promoted $Zn_1Zr_8O_n$ catalyst was also observed with respect to its binary $Zn_1Zr_8O_n$ counterpart. The choice of A-site metal is of prime importance in the isobutene production, catalyzing mainly the ethanol dehydrogenation, meanwhile the appropriate addition of zinc on the catalyst surface is also essential for good isobutene yield.

Keywords

1. Introduction

Conversions from sustainable biomass-based raw materials to valuable fuels and chemicals have drawn intensive interest to meet grand challenges in global warming and depletion of fossil feedstocks [1] [2]. With the development of biological fermentation, bio-ethanol has become the major product from biomass conversion [3] [4]. Currently, bio-ethanol conversions to highly valuable chemicals are mainly focused on ethanol dehydration to ethylene over solid acid catalysts, such as alumina [5], zeolites [6] and heteropoly acids [7] or ethanol dehy-

---

*Corresponding author.

drogenation to acetaldehyde and then to acetone *via* aldol-condensation routes [8]. In particular, bio-ethanol conversion to lighter olefins has become a strategic reaction for the production of highly valuable chemicals. At present, isobutene is predominantly produced *via* extractive distillation of the C_4 fraction from catalytic steam cracking of fossil-based naphtha in ethylene production. With the switching to shale gas for industrial production of ethylene, it calls for alternative methods of C_4 light olefins synthesis. Therefore, it is highly desirable to explore new routes to produce isobutene from renewable resources.

Tago *et al.* [9] found that alkali metal ion-exchanged BEA zeolites exhibited the high yield (55%) of acetone conversion to isobutene as a result of elimination of the strong acidic sites by introduced alkali metal ions (Na, K, Rb and Cs) and inhibition of the formation of aromatics and coke. Wang and co-workers reported the first evidence of direct conversion of bio-ethanol to isobutene (ETIB) over $Zn_xZr_yO_z$ mixed oxide catalyst [10]. They rationalized that the balanced acid-base sites of $Zn_xZr_yO_z$ were responsible for the direct and high-yield conversion of ETIB. The direct one-step conversion of ethanol to value-added C_4 light olefins has long been the target of catalysis research [11]. SiO_2-MgO mixed oxides have been found to be active for one-step conversion of ethanol to 1,3-butadiene, and with various dopants introduced, such as Cu [12], Ag [13], and other transition metal (oxide)s [14]. The catalytic properties of the binary SiO_2-MgO system can be enhanced by promoting the dehydrogenation of ethanol and by shifting the rate-relevant step of the reaction network.

In this work, different A-site metals such as Fe, Cr, and Ni were introduced into binary $Zn_1Zr_8O_n$ forming ternary $A_1Zn_1Zr_8O_n$ composite catalysts, aiming to enhance the catalytic activity for ETIB reaction. Our results show that by introducing Cr, the selectivity of isobutene formation over ternary $Cr_1Zn_1Zr_8O_n$ mixed oxide composite is markedly increased compared to that of binary $Zn_1Zr_8O_n$. Meanwhile, the contents of zinc and zirconium species were found to be essential for the isobutene production over ternary $Cr_1Zn_yZr_zO_n$.

2. Experimental

2.1. Preparation of Ternary $A_1Zn_yZr_zO_n$ Catalysts

To synthesize ternary $A_1Zn_yZr_zO_n$ catalysts, we employed the conductive carbon black T100 as the hard template, which was heated at 180°C overnight before being used. In a typical synthesis, 0.00125 mol of $Zn(NO_3)_2 \cdot 6H_2O$ (Sigma-Aldrich, >99.8%), 0.01 mol of $ZrO(NO_3)_2 \cdot xH_2O$ (Sigma-Aldrich, >99.8%), and 0.00125 mol of $Ni(NO_3)_2 \cdot 3H_2O$ (Sigma-Aldrich, >99.8%) were dissolved in 40 ml de-ionized water with ultrasonic treatment for 30 mins to obtain a clear and homogeneous solution. Then, 6.0 g of preheated MA100 (Mitsubishi, Japan) was added into the above solution with stirring at the speed of 500 RPM for 2.0 hrs. After that, the mixture was transferred to a ceramic crucible and dried at 110°C for 12 hrs in oven and further calcined at 400°C for 4.0 hrs and stay at 550°C for another 20 hrs to remove the carbon black. The obtained white powders were denoted as $Ni_1Zn_1Zr_8O_n$ catalysts. When $Ni(NO_3)_2 \cdot 3H_2O$ was replaced by $Fe(NO_3)_3 \cdot 9H_2O$, $Co(NO_3)_2 \cdot 3H_2O$ or $Cr(NO_3)_3 \cdot 9H_2O$, $Fe_1Zn_1Zr_8O_n$, $Co_1Zn_1Zr_8O_n$ or $Cr_1Zn_1Zr_8O_n$ composite oxide was obtained, respectively.

2.2. Catalyst Characterizations

Several physical techniques were employed to characterize the structure of synthesized catalysts. a) X-ray powder diffraction patterns (XRD) for all the samples were collected on X-ray diffractometer. b) Morphology and size of $Cr_1Zn_1Zr_8O_n$ catalyst were probed by field emission scanning electron microscopy (FESEM, Hitachi S4800). c) Nitrogen adsorption-desorption isotherms were recorded on a Micromeritics ASAP 2460 at 77 K, where the specific surface areas (S_{BET}), pore volume (V_P) and pore diameter (D_P) were calculated by applying the Brunauer-Emmett-Teller (BET) and Barrett-Joyner-Halenda (BJH) models to the desorption branches.

2.3. Catalytic Activity Measurements

The vapor-phase ETIB reactions were evaluated in a tubular quartz reactor (i.d. 5.0 mm). In each run, 200 mg catalyst pelletized catalyst sample (size range: 40 - 60 mesh) was placed at the center of the reactor tube between two layers of quartz wool and were pretreated in N_2 (50 ml/min) at 400°C for 0.5 h. A mixture of ethanol/H_2O (steam/carbon ratio = 5.0) was then introduced into the evaporator (200°C) by a syringe pump and directly carried into the reaction system by flowing carrier gas of N_2. An online Shimadzu 2014 Gas Chromatography (GC) with three analyzing channels was used for full product analysis. The carbon balance was checked in each run and found to be higher than 95% in every case. The ethanol conversion and product selectivity were calculated on a per carbon basis and defined by two following equations:

$$\text{conversion} = \frac{\text{Ethanol}_{\text{in}} - \text{Ethanol}_{\text{out}}}{\text{Ethanol}_{\text{in}}} \times 100\% \tag{1}$$

$$\text{Swlectivity} = \frac{\text{Carbon in given product}}{\text{Carbon in all products}} \times 100\% \tag{2}$$

3. Results and Discussions

3.1. Catalyst Characterization

3.1.1. XRD

Figure 1 displays XRD profiles of ternary $A_1Zn_1Zr_8O_n$ composite oxides in the comparison with binary $Zn_1Zr_8O_n$. Tetragonal phase of ZrO_2 (PDF#50-1089) are observed for all samples. But the details of the diffraction peaks change greatly with different A-site dopants. Binary $Zn_1Zr_8O_n$ only shows diffraction peaks from tetragonal phase of ZrO_2. Sharper diffraction peaks of tetragonal ZrO_2 are found over $Ni_1Zn_1Zr_8O_n$, and some diffraction peaks assignable to NiO (PDF#2901) are obvious. The introduction of Fe did not affect the diffraction peaks of tetragonal ZrO_2. $Co_1Zn_1Zr_8O_n$ shows the weak diffraction peaks of CoO species (PDF#2902) and the peaks belonging to tetragonal ZrO_2 remained unchanged. Although additional diffraction peaks are not found after introducing Cr, it is noted that diffraction peaks of tetragonal ZrO_2 are weakened. So, when binary $Zn_1Zr_8O_n$ composite oxides dope with a little of transition metal species, the changes depend on dopants. The introduction of Fe and Co species cannot affect the crystallinity. An opposite effection of the crystallinity is found when Ni and Cr are added. When Ni and Co are introduced, highly dispersed Ni and Co species were not formed. In this case, the bulk phase of NiO and CoO was formed in there two catalysts.

3.1.2. N_2 Adsorption-Desorption

Figure 2 shows that all the catalysts display the type IV N_2 absorption-desorption isotherms with H3 hysteresis loops at the relative pressure (P/P_0) ranging from 0.80 to 1.0, an indicative of a typical mesoporous structure. This indicates that the porous structure is not destroyed by doping. We also have calculated BET surface area (S_{BET}), pore volume (V_P) and pore diameter (D_P) from N_2 absorption-desorption isotherms using BET and BJH models, and the results are shown in **Table 1**. It can be seen that only introducing Cr improves the S_{BET} while other dopants introduced into the binary $Zn_1Zr_8O_n$ will cause the decrease of specific surface area.

3.1.3. FESEM

Figure 3 presents the FESEM chemical mapping image, which definitely shows the homogeneous distribution
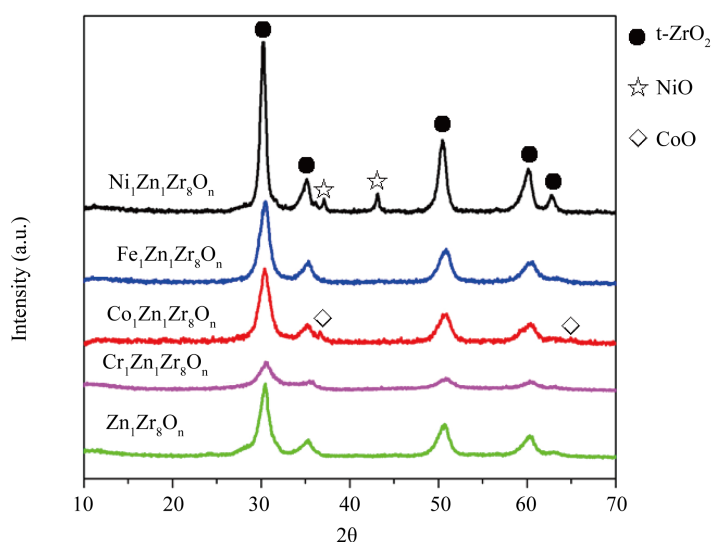

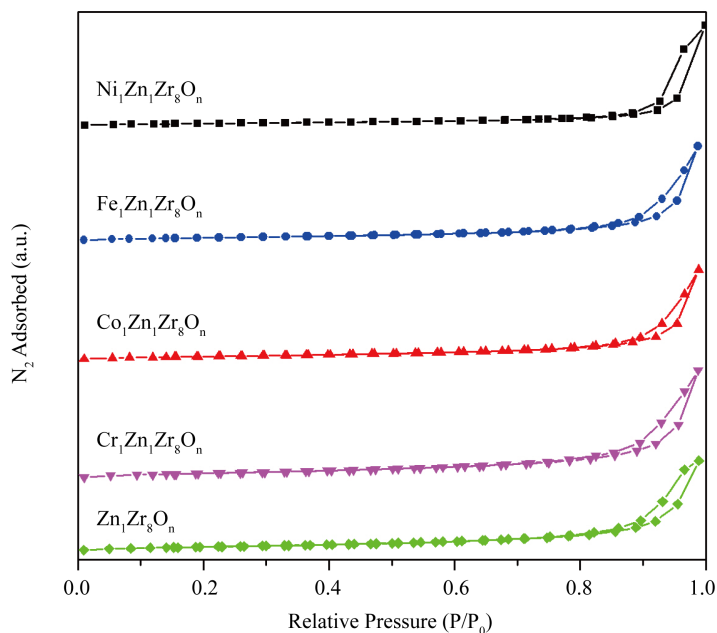**Figure 1.** XRD patterns of $A_1Zn_1Zr_8O_n$ and $Zn_1Zr_8O_n$ catalysts.

Figure 2. N_2 adsorption-desorption isotherms of $A_1Zn_1Zr_8O_n$ and $Zn_1Zr_8O_n$ catalysts.

Table 1. Physical and chemical properties of $A_1Zn_1Zr_8O_n$ catalysts.

Catalysts	S_{BET} (cm^2/g)	V_p (cm^3/g)	D_p (nm)	Crystallite size (nm)
$Ni_1Zn_1Zr_8O_n$	60.9	0.18	10.47	12.7
$Fe_1Zn_1Zr_8O_n$	87.5	0.60	10.50	9.3
$Co_1Zn_1Zr_8O_n$	87.7	0.57	9.47	9.2
$Cr_1Zn_1Zr_8O_n$	125.4	0.69	9.60	10.0
$Zn_1Zr_8O_n$	106.6	0.43	8.19	10.6
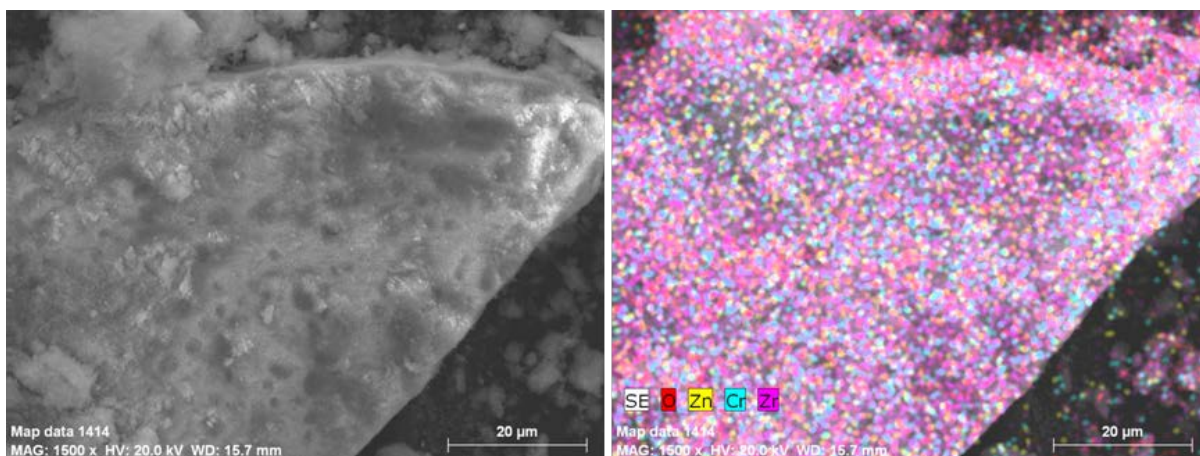
Figure 3. FESEM images corresponding element mapping of $Cr_1Zn_1Zr_8O_n$ catalyst.

of Cr and Zn atoms with Zr and O atoms as a background, which support XRD results that the synthesized mixed metal oxides contain no individual Cr_2O_3 or ZnO phase.

3.2. Catalytic Performances

Figure 4 presents the product distributions of ETIB reaction over ternary $A_1Zn_1Zr_8O_n$ and binary $Zn_1Zr_8O_n$ catalysts at 500°C. One can see that the selectivity of isobutene is 37 % and 39% CO_2 is gained on binary $Zn_1Zr_8O_n$ catalysts. AsNi and Co is introduced forming $Ni_1Zn_1Zr_8O_n$ and $Co_1Zn_1Zr_8O_n$, respectively. There are no notable changes of product distribution with respect to binary $Zn_1Zr_8O_n$. But only acetone selectivity decreases or increases. When Fe is introduced forming $Fe_1Zn_1Zr_8O_n$, isobutene selectivity (8%) decreased dramatically which is far below binary $Zn_1Zr_8O_n$. In this case a lot of CO_2 (62%) is generated, suggesting that the Fe species favors hydrogen production via steam reforming of ethanol ($CH_3CH_2OH + H_2O \rightarrow CO_2 + H_2$). A large amount of H_2 obtained in product effluents also supports this argument. In all ternary catalysts, $Cr_1Zn_1Zr_8O_n$ shows the best isobutene selectivity (51%), while the acetone selectivity increases to 12% and CO_2, CH_4 and ethylene selectivity decreases to 30%, 0.7% and 0.9% respectively, suggesting that ethanol dehydration and cracking are suppressed.

Reaction condition: catalyst weight m = 0.20 g; S/C = 5; $x_{ethanol}$ = 2.73 mol% (N_2 balance); W/F = 0.0975 $g \cdot s \cdot ml^{-1}$, P = 1 atm., T = 500°C.

As can be seen from **Figure 5**, the content of ZnO notably affected the product distribution of bioethanol conversion at 500°C. When y value varies from 0 to 1, ethylene selectivity decreases and isobutene selectivity increases greatly. At the same time, acetone selectivity increases firstly and then decreases. At y = 2, isobutene selectivity decreases and ethylene shows up again. This suggests that the appropriate content of the zinc addition is very important to the good isobutene selectivity.

From above, we can conclude that the functionalized active sites associated with A, Zn and Zr content in $A_1Zn_yZr_zO_n$ catalyst should be well matched to obtain the highest isobutene selectivity in ETIB reaction. Although the first step, ethanol dehydrogenation is not a difficult reaction, there is still the intense competition between ethanol dehydrogenation and dehydration. The introduction of transition metal species such as Cr can significantly promote the dehydrogenation and suppress the parallel competitive dehydration. The next steps (acetaldehyde-to-acetone and acetone-to-isobutene) need a proper balance between acid and basic sites, which have been evidenced by appropriate Zn addition. Because of the presence of single oxide, which is badly cooperated with other active sites, the introduction of Co or Ni cannot gain better isobutene selectivity. Especially, the introduction of Fe breaks the reaction path and leads to more by-products. Since ZnO is amphoteric oxide, and the excess or the insufficient of its addition will lead to other side reactions and cannot obtain good isobutene selectivity.
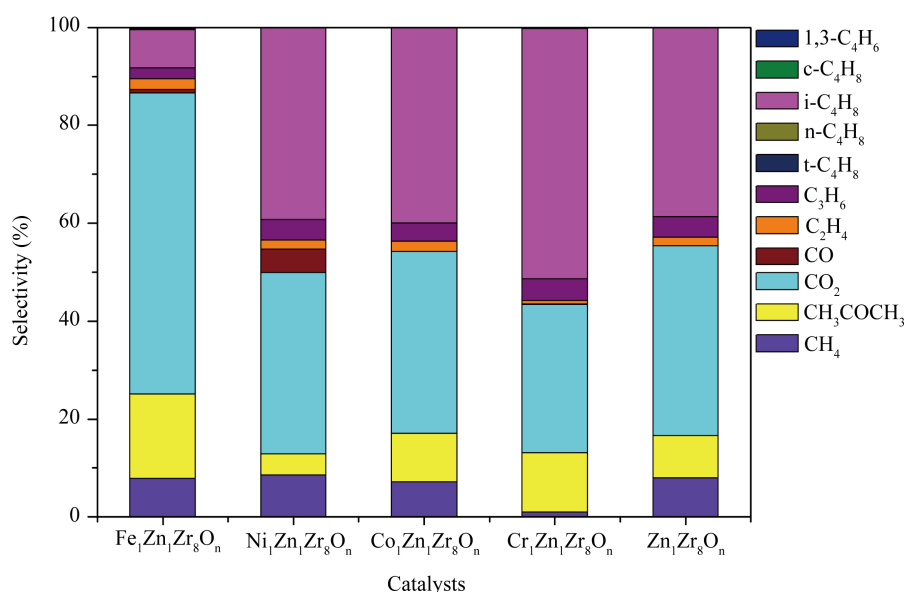

Figure 4. Product distribution of bio-ethanol conversion over $A_1Zn_1Zr_8O_n$ and $Zn_1Zr_8O_n$ catalysts. Reaction condition: catalyst weight m = 0.20 g; S/C = 5; $x_{ethanol}$ = 2.73 mol % (N_2 balance); W/F = 0.0975 $g \cdot s \cdot ml^{-1}$, P = 1 atm., T = 500°C.

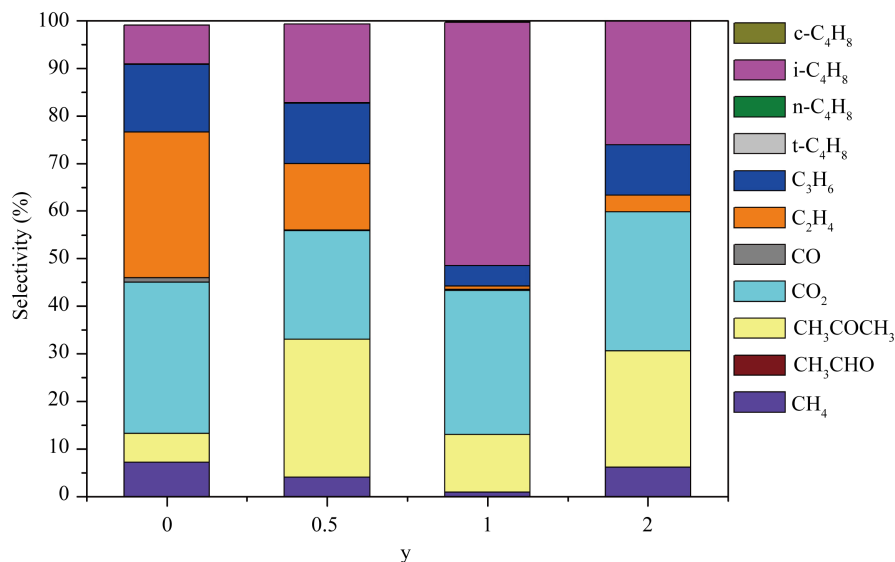**Figure 5.** Product distribution of bioethanol conversion over $Cr_1Zn_yZr_8O_n$ catalysts. Reaction condition: catalyst weight m = 0.20 g; S/C = 5; $x_{ethanol}$ = 2.73 mol % (N_2 balance); W/F = 0.0975 g·s·ml^{-1}, P = 1 atm., T = 500°C.

4. Conclusion

A series of ternary $A_1Zn_yZr_zO_n$ catalysts using hard template method were synthesized and investigated for the activity of direct ETIB. Introduction of transition metal species into A-site of $Zn_yZr_zO_n$ significantly affected the catalytic reactivity. In particular, introduction of Cr species into $Zn_1Zr_8O_n$ is essential for promoting ETIB activity with respect to binary $Zn_1Zr_8O_n$ which is closely related to excellent ethanol dehydrogenation capability caused by its redox properties. Meanwhile, appropriate addition of zinc on the catalyst surface is also essential for good isobutene yield. On the whole, the species and the quantity of active sites are the key to the target product isobutene.

Acknowledgements

References

[1] Chheda, J.N., Huber, G.W. and Dumesic, J.A. (2007) Liquid-Phase Catalytic Processing of Biomass-Derived Oxygenated Hydrocarbons to Fuels and Chemicals. *Angewandte Chemie International Edition*, **46**, 7164-7183.
http://dx.doi.org/10.1002/anie.200604274

[2] Limayem, A. and Ricke, S.C. (2012) Lignocellulosic Biomass for Bioethanol Production: Current Perspectives, Potential Issues and Future Prospects. *Progress in Energy & Combustion Science*, **38**, 449-467.
http://dx.doi.org/10.1016/j.pecs.2012.03.002

[3] Alvira, P., Tomás-Pejó, E., Ballesteros, M. and Negro, M.J. (2010) Pretreatment Technologies for an Efficient Bioethanol Production Process Based on Enzymatic Hydrolysis: A Review. *Bioresource Technology*, **101**, 4851-4861.
http://dx.doi.org/10.1016/j.biortech.2009.11.093

[4] Hahn-Hägerdal, B., Galbe, M., Gorwa-Grauslund, M.F., Lidén, G. and Zacchi, G. (2006) Bio-Ethanol—The Fuel of Tomorrow from the Residues of Today. *Trends in Biotechnology*, **24**, 549-556.
http://dx.doi.org/10.1016/j.tibtech.2006.10.004

[5] Chen, G., Li, S., Jiao, F. and Yuan, Q. (2007) Catalytic Dehydration of Bioethanol to Ethylene over TiO_2/γ-Al_2O_3 Cat-

alysts in Microchannel Reactors. *Catalysis Today*, **125**, 111-119. http://dx.doi.org/10.1016/j.cattod.2007.01.071

[6] Han, Y., Lu, C., Xu, D., Zhang, Y., Yi, H. and He, H. (2011) Molybdenum Oxide Modified HZSM-5 Catalyst: Surface Acidity and Catalytic Performance for the Dehydration of Aqueous Ethanol. *Applied Catalysis A General*, **396**, 8-13. http://dx.doi.org/10.1016/j.apcata.2010.12.040

[7] Varisli, D., Dogu, T. and Dogu, G. (2009) Novel Mesoporous Nanocomposite WOx-Silicate Acidic Catalysts: Ethylene and Diethylether from Ethanol. *Industrial & Engineering Chemistry Research*, **48**, 9394-9401. http://dx.doi.org/10.1021/ie8008154

[8] Nakajima, T., Tanabe, K., Yamaguchi, T., Matsuzaki, I. and Mishima, S. (1989) Conversion of Ethanol to Acetone over Zinc Oxide—Calcium Oxide Catalyst Optimization of Catalyst Preparation and Reaction Conditions and Deduction of Reaction Mechanism. *Applied Catalysis*, **52**, 237-248. http://dx.doi.org/10.1016/0166-9834(89)80006-5

[9] Tago, T., Konno, H., Ikeda, S., Yamazaki, S., Ninomiya, W., Nakasaka, Y., Masuda, T., Konno, H., Ikeda, S. and Yamazaki, S. (2011) Selective Production of Isobutylene from Acetone over Alkali Metal Ion-Exchanged BEA Zeolites. *Catalysis Today*, **164**, 158-162. http://dx.doi.org/10.1016/j.cattod.2010.10.034

[10] Sun, J., Zhu, K., Gao, F., Wang, C., Liu, J., Peden, C.H. and Wang, Y. (2011) Direct Conversion of Bio-Ethanol to Isobutene on Nanosized Zn(x)Zr(y)O(z) Mixed Oxides with Balanced Acid-Base Sites. *Journal of the American Chemical Society*, **133**, 11096-11099. http://dx.doi.org/10.1021/ja204235v

[11] Sun, J. and Wang, Y. (2014) Recent Advances in Catalytic Conversion of Ethanol to Chemicals. *ACS Catalysis*, **4**, 1078-1090. http://dx.doi.org/10.1021/cs4011343

[12] Angelici, C., Velthoen, M.E.Z., Weckhuysen, B.M. and Bruijnincx, P.C.A. (2014) Effect of Preparation Method and CuO Promotion in the Conversion of Ethanol into 1,3-Butadiene over SiO$_2$-MgO Catalysts. *Chemsuschem*, **7**, 2505-2515. http://dx.doi.org/10.1002/cssc.201402361

[13] Janssens, W., Makshina, E.V., Vanelderen, P., Houthoofd, K., Kerkhofs, S., Martens, J.A., Jacobs, P.A. and Sels, B.F. (2015) Ternary Ag/MgO:SiO$_2$ Catalysts for the Conversion of Ethanol into Butadiene. *Chemsuschem*, **8**, 913-913. http://dx.doi.org/10.1002/cssc.201500081

[14] Makshina, E.V., Janssens, W., Sels, B.F. and Jacobs, P.A. (2012) Catalytic Study of the Conversion of Ethanol into 1,3-Butadiene. *Catalysis Today*, **198**, 338-344. http://dx.doi.org/10.1016/j.cattod.2012.05.031